

Effects of palmitoylation on membrane protein partitioning into lipid domains in model cellular membranes

Shishi Wu(吴施施) and Qing Liang(梁清)

Citation: Chin. Phys. B, 2025, 34 (**5**): 058701. DOI: 10.1088/1674-1056/adbee9
http://cpb.iphy.ac.cn; http://iopscience.iop.org/cpb

What follows is a list of articles you may be interested in

Improving performance of screening MM/PBSA in protein-ligand interactions via machine learning

Yuan-Qiang Chen(陈远强), Yao Xu(徐耀), Yu-Qiang Ma(马余强), and Hong-Ming Ding(丁泓铭)
Chin. Phys. B, 2025, 34 (**1**): 018701. DOI: 10.1088/1674-1056/ad8ecb

Subtraction of liposome signals in cryo-EM structural determination of protein-liposome complexes

Shouqing Li(李首卿), Ming Li(李明), Yumei Wang(王玉梅), and Xueming Li(李雪明)
Chin. Phys. B, 2024, 33 (**8**): 088702. DOI: 10.1088/1674-1056/ad4cdb

Factors resisting protein adsorption on hydrophilic/hydrophobic self-assembled monolayers terminated with hydrophilic hydroxyl groups

Dangxin Mao(毛党新), Yuan-Yan Wu(吴园燕), and Yusong Tu(涂育松)
Chin. Phys. B, 2024, 33 (**6**): 068701. DOI: 10.1088/1674-1056/ad39ca

Origin of tradeoff between movement velocity and attachment duration of kinesin motor on a microtubule

Yuying Liu(刘玉颖) and Zhiqiang Zhang(张志强)
Chin. Phys. B, 2024, 33 (**2**): 028708. DOI: 10.1088/1674-1056/ad1177

Unraveling the molecular mechanism of prion disease: Insights from α2 area mutations in human prion protein

Rongri Tan(谈荣日), Kui Xia(夏奎), Damao Xun(寻大毛), Wenjun Zong(宗文军), and Yousheng Yu(余幼胜)
Chin. Phys. B, 2023, 32 (**12**): 128703. DOI: 10.1088/1674-1056/ad08a8

Effects of palmitoylation on membrane protein partitioning into lipid domains in model cellular membranes

Shishi Wu(吴施施)[1,2] and Qing Liang(梁清)[1,2,†]

[1] *Department of Physics, Zhejiang Normal University, Jinhua* 321004, *China*
[2] *Zhejiang Institute of Photoelectronics & Zhejiang Institute for Advanced Light Source, Zhejiang Normal University, Jinhua* 321004, *China*

(Received 31 January 2025; revised manuscript received 5 March 2025; accepted manuscript online 11 March 2025)

The partitioning of membrane proteins into lipid domains in cellular membranes is closely associated with the realization of the protein functions and it is influenced by various factors such as the post-translational modification of palmitoylation. However, the molecular mechanism of the effect of palmitoylation on membrane protein partitioning into the lipid domains remains elusive. In this work, taking human peripheral myelin protein 22 (PMP22) as an example, we employ coarse-grained molecular dynamics simulations to investigate the partitioning of both the natural PMP22 and the palmitoylated PMP22 (pal-PMP22) into the lipid domains of model myelin membranes. The results indicate that palmitoylation drives PMP22 to localize at the boundary of the liquid-ordered (Lo) and liquid-disordered (Ld) domains and increases the possibility of PMP22 partitioning into the Lo domains by changing the hydrophobic length of the proteins and perturbing the ordered packing of tails of the saturated lipids in the Lo domains. This work offers some novel insights into the role of palmitoylation in modulating the function of membrane proteins in cellular membranes.

Keywords: protein, palmitoylation, lipid domain, molecular simulation

PACS: 87.14.E–, 87.15.–v, 87.16.dt, 87.15.ap

DOI: 10.1088/1674-1056/adbee9 **CSTR:** 32038.14.CPB.adbee9

1. Introduction

The composition of plasma membranes is highly complex, composed of thousands of different lipids and various membrane proteins.[1] Due to distinct physicochemical properties, lipids segregate into nanosized domains with unique characteristics under physiological conditions.[2] For instance, lipid rafts represent a typical type of liquid-ordered (Lo) domains enriched in saturated lipids, cholesterol (CHOL), and specific proteins.[3,4] In contrast, liquid-disordered (Ld) domains, enriched with unsaturated lipids, are another key feature of plasma membranes. The distribution of membrane proteins across these lipid domains is closely associated with the biological functions of the membrane proteins and the properties of the domains themselves.[5–7] Previous studies have found that many membrane proteins prefer to partition into lipid rafts or Lo domains in the natural plasma membranes or the giant plasma membrane vesicles (GPMVs) while they preferentially partition into Ld domains in simplified model cellular membranes such as the giant unilamellar vesicle (GUV) composed of ternary lipids of saturated lipids, unsaturated lipids, and CHOL.[8–14] These findings suggest that the partitioning of membrane proteins into lipid domains in plasma membranes is rather complicated and may involve many factors.

Human peripheral myelin protein 22 (PMP22) is a membrane glycoprotein playing key roles in the formation of myelin and CHOL homeostasis in the peripheral myelin sheath.[15–19] As one of the major myelin proteins, PMP22 is tightly linked to a variety of peripheral myelin nerve diseases, including Charcot–Marie–Tooth (CMT) disease,[20] hereditary neuropathy with liability to pressure palsies,[21] and inflammatory demyelinating polyneuropathy,[22] through mutations or abnormal expressions.[23]

As a membrane protein, the function of PMP22 is primarily regulated by its interactions with lipids in the myelin membrane.[24,25] Particularly, the partitioning of PMP22 into the lipid domains has a significant impact on the functions of the protein. It has been found that PMP22 preferentially partitions into Lo domains in the myelin membrane, whereas mutations may change the PMP22 partitioning into the lipid domains, leading to diseases.[20,26,27] On the contrary, PMP22 may also influence the lateral organization of lipids in the myelin membrane.[28,29] For example, the over-expression of PMP22 has been shown to disturb the ordered packing of lipids in the myelin membrane, affecting the membrane stability and the myelin function.[19] However, the microscopic mechanism dominating the PMP22 partitioning into the lipid domains are still poorly understood.

Palmitoylation is a crucial post-translational modification that plays a key role in the functions of PMP22.[30] In the palmitoylation of PMP22, the palmitic acid chain is covalently grafted to the cysteine at residue 85.[30,31] Recently,

†Corresponding author. E-mail: qliang@zjnu.edu.cn

© 2025 Chinese Physical Society and IOP Publishing Ltd. All rights, including for text and data mining, AI training, and similar technologies, are reserved.

it has been shown that both PMP22 and the palmitoylated PMP22 (pal-PMP22) prefer to partition into Lo domains in the GPMVs derived from the natural myelin membranes, indicating that palmitoylation has no obvious impact on the partitioning of PMP22 in the lipid domains in the natural myelin membrane.[26] However, in the ternary GUV composed of palmitoyloleoyl-phosphocholine (POPC), palmitoylsphingomyelin (PSM), and CHOL, the natural PMP22 was found to preferentially partition into Ld domains.[32] Although there is no direct evidence of the effects of palmitoylation on the partitioning of PMP22 into lipid domains in GUV systems, experiments have shown that palmitoylation significantly affects the partitioning of other proteins in these systems, driving them from the Ld domains to the Lo domains.[33,34] Therefore, palmitoylation may also exhibit varying effects on the partitioning of PMP22 into lipid domains across different membranes, and it may be a crucial driving force for the partitioning of pal-PMP22 into the lipid rafts in the natural myelin membranes. Despite these efforts, the microscopic mechanism by which palmitoylation affects the partitioning of PMP22 into lipid domains remains elusive.

In this study, we investigate how palmitoylation affects the partitioning of PMP22 into the lipid domains in model myelin membranes by employing coarse-grained molecular dynamics (MD) simulations.[35,36] Our results show that the effect of palmitoylation on the partitioning of PMP22 into the lipid domains varies in model myelin membranes composed of different lipids. In the ternary lipid bilayers composed of saturated dipalmitoyl–phosphatidylcholine (DPPC), unsaturated dilinoleoyl–phosphatidylcholine (DIPC), and CHOL, palmitoylation exhibits an obviously facilitating effect on the localization of PMP22 at the boundary of the Lo and Ld domains. However, in the lipid bilayers composed of DPPC, dioleoyl–phosphatidylcholine (DOPC), and CHOL, the effect of palmitoylation on the partitioning of PMP22 into the lipid domains is negligible. We further reveal the microscopic mechanism of the effect of palmitoylation on the partitioning of PMP22 into the lipid domains from the thermodynamic perspective, providing the molecular insights into PMP22 partitioning into lipid rafts in the natural myelin membranes.

2. Model and methods

2.1. System setup

To study the interaction between PMP22 and myelin membranes, we used coarse-grained Martini 3 force field to build the molecular simulation models.[37,38] The Martini force field has been successfully used to investigate the phase separation and protein–lipid interactions in cellular membranes.[39–43] Compared with Martini 2, the latest Martini 3 introduces new bead types to reduce the excessive hydrophobicity and self-interactions of proteins encountered in Martini 2.[35,38]

2.1.1. Proteins

Since the crystal structure of PMP22 has not yet been resolved experimentally, we adopted the computed PMP22 structure (AlphaFoldDB: Q01453) released by AlphaFold2 for the simulations.[44,45] The amino acid sequence of PMP22 is shown in Fig. 1(a). The palmitoylation of PMP22 was realized by the online tool CHARMM-GUI (https://www.charmm-gui.org/).[46] The coarse-grained structure of the proteins were obtained by using the scripts of martinize2 provided by the Martini force field developers. The palmitoylation of PMP22 was described by the coarse-grained Martini 3 force field developed by Koukos *et al.*[47] The coarse-grained molecular structures of the natural PMP22 and the pal-PMP22 are illustrated in Fig. 1(b). In the pal-PMP22, the palmitic acid chain is covalently linked to the cysteine at residue 85 (CYS85) according to the experimental structure.[30]

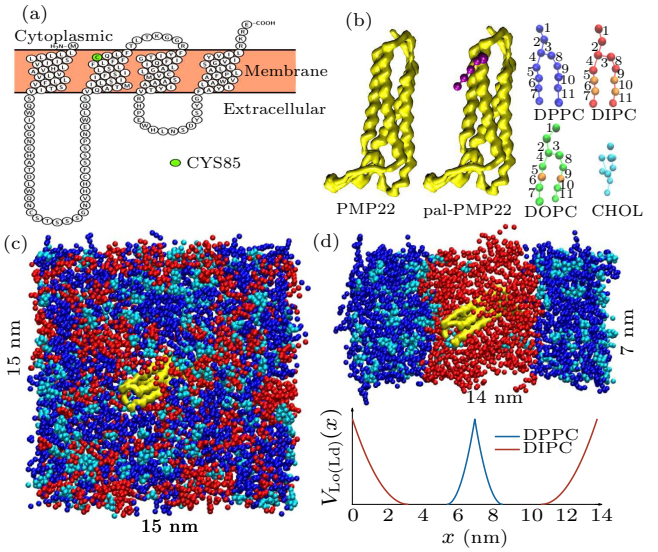


Fig. 1. (a) The amino acid sequence of PMP22, with the palmitoylation site (CYS85) highlighted in green. (b) The coarse-grained structures of proteins of PMP22 and pal-PMP22 with the palmitic acid chain shown in purple, and the coarse-grained structures of the lipids used in this work. Here, the positions of the unsaturated double bonds in the lipid tails are shown in orange. The number of the bond is labeled for the convenience of the calculation of the order parameter of the lipid tails. (c) The structure of a lipid bilayer composed of DPPC (blue), DIPC (red), CHOL (cyan) with a PMP22 protein inserted. (d) The structure of a pre-separated Lo–Ld–Lo lipid bilayer (top) composed of DPPC, DIPC, and CHOL and inserted with a PMP22 protein, with flat-bottom potentials (bottom) imposed on DPPCs (blue) and DIPCs (red), respectively.

2.1.2. Lipid bilayers

Using the tool of INSANE developed by Martini group,[48] we constructed two kinds of ternary lipid bilayers composed of 274 DPPCs, 205 DIPCs or DOPCs, and 205 CHOLs with the molar ratio of 4:3:3. The coarse-grained molecular structures of the lipids are shown in Fig. 1(b). Here, DPPC is the fully saturated lipid, while DIPC and DOPC are unsaturated lipids with two and one unsaturated double

bond(s) per fatty acid tail, respectively. The structure of a lipid bilayer composed of DPPC, DIPC, and CHOL is shown in Fig. 1(c). At the simulation temperature (300 K) in this work, both the lipid bilayers spontaneously segregate into Lo domains enriched in DPPC and CHOL and Ld domains enriched in DIPC or DOPC.[41,49] Additionally, the physiological environments of the lipid bilayers were mimicked using the explicit coarse-grained water molecules and 0.15-M sodium chloride (NaCl).

2.2. Simulation protocol

The coarse-grained MD simulations were performed using the GROMACS (version 2019.7) package.[50] In the simulations, the nonbonded electrostatic interaction was shifted to zero within 0 nm–1.2 nm, and the Lennard–Jones interaction was shifted to zero between 0.9 nm and 1.1 nm. All simulations were implemented using the isothermal–isobaric (NpT) ensemble with constant particle number, pressure, and temperature. A velocity-rescaling thermostat with a time coupling constant of 1 ps was used to maintain the temperature at 300 K.[51] The pressure was maintained at 1 bar (1 bar = 10^5 Pa) in both the bilayer plane (xy) and the bilayer normal (z) directions using a semi-isotropic Berendsen barostat with a time coupling constant of 1 ps.[52] Periodic boundary conditions were applied in all three directions. The integration time step for the MD simulations was 20 fs and each simulation was run for a total length of 20 μs.

2.3. Calculation of PMF of PMP22/pal-PMP22 in different lipid domains

To elucidate the interactions between PMP22/pal-PMP22 and the Lo/Ld domains from the thermodynamic perspective, we calculated the potential of mean force (PMF) using the umbrella sampling method. For the convenience of the PMF calculation, as shown in Fig. 1(d), we constructed a pre-separated lipid bilayer with an Lo–Ld–Lo structure by restraining the lateral diffusion of the lipids through an inverted flat-bottom harmonic potential[53]

$$V_{\mathrm{Lo(Ld)}}(x)=\begin{cases}\dfrac{k(|x-x_{\mathrm{c}}|-d/2)^2}{2}, & \text{if} \quad |x-x_{\mathrm{c}}|-d/2<0;\\ 0, & \text{if} \quad |x-x_{\mathrm{c}}|-d/2\geq 0.\end{cases} \tag{1}$$

Here, $k=500$ kJ·mol^{-1}·nm^{-2} is the force constant of the potential, x_{c} is the lateral coordinate of the center of the lipid domains in the x direction, and d is the width of the lipid domains in the x direction. For the Lo domain, x_{c} is located at the center of the simulation box in the x direction, while for the Ld domain, x_{c} is located at the boundary of the simulation box.[54] It is notable that the inverted flat-bottom potential is only imposed on DPPC in the Lo domain and DIPC or DOPC in the Ld domain while the CHOL molecules were not restrained. The Lo domain consists of 160 DPPCs and 120 CHOLs with the molar ratio of 4:3 while the Ld domain is composed of 94 pure DIPCs or DOPCs.

In the umbrella sampling simulation, the x coordinate of the protein was chosen as the reaction coordinate and the simulation windows were produced by the pulling simulation with an interval of 0.1 nm. The protein was restrained by a harmonic potential with a force constant of 1000 kJ·mol^{-1}·nm^{-2} in each window. Each window was simulated for 500 ns and the last 200-ns trajectory was used to calculate the PMF profile using the weighted histogram analysis method (WHAM) with the *gmx wham* tool in the package of GROMACS.[55,56] Addtionally, the errors of the PMF were estimated using the bootstrapping method.[56,57] To estimate the convergence of the PMF, the simulation trajectory of the last 200 ns was divided into several segments to compare the PMF profile.[58]

2.4. Data analysis

The visualization of the MD trajectories was realized using the software of Visual Molecular Dynamics (VMD).[59] The number of contact between the protein and lipids was calculated using the *gmx mindist* tool with a cutoff distance 0.5 nm in the GROMACS package. Additionally, the contact map was derived from data obtained by calculating the number of contacts between each amino acid and the lipids using the same tool. The order parameter ($P_z=\frac{1}{2}(3\cos^2\theta-1)$) of the lipid tail chains was calculated using the scripts developed by the Martini group. Here, θ is the averaged angle between the bond in the lipid tails and the bilayer normal. $P_z=1$ represents the lipid tails aligning perfectly parallel with the bilayer normal, $P_z=0$ represents the random packing of the lipid tails, and $P_z=-0.5$ represents the anti-parallel alignment of the lipid tails with the bilayer normal.

3. Results and discussion

3.1. Partitioning of PMP22/pal-PMP22 into lipid domains

Figure 2(a) shows the distribution of PMP22 in the lipid bilayers composed of DPPC, DIPC, and CHOL in the 20-μs simulation. We find that, in most of the simulation time, PMP22 either partitions into the Ld domain enriched in DIPC or localizes near the boundary of the Lo and Ld domains, but it is not found to partition into the Lo domain enriched in DPPC and CHOL. This result agrees with the experimental results of the partitioning of PMP22 in the GUV composed of simple ternary lipids.[32] However, in the GPMV extracted from the Hela cell, PMP22 was found to preferentially partition into the Lo domains, which is not consistent with our simulation results.[26] Therefore, the compositional complexity of the lipid bilayers has a significant effect on the partitioning of PMP22 into the lipid domains.

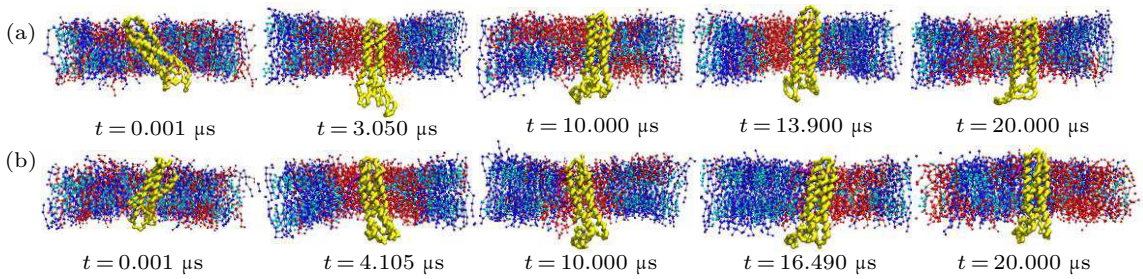


Fig. 2. Representative snapshots for the partitioning of (a) PMP22 and (b) pal-PMP22 into the lipid domains in the lipid bilayer composed of DPPC (blue), DIPC (red), and CHOL (cyan) in the 20-μs simulations.

To elucidate the effect of palmitoylation on the partitioning of PMP22 into the lipid domains, we further examine the partitioning of pal-PMP22 in the DPPC/DIPC/CHOL bilayer and the simulation results are shown in Fig. 2(b). The results indicate that pal-PMP22 localizes near the boundary of the Lo and Ld domains in most of the simulation time. However, it is found that the palmitoylation site is always in contact with saturated lipids and CHOL, even when pal-PMP22 partitions into the Ld domains. In the lipid bilayer of DPPC/DOPC/CHOL, the partitioning of PMP22 and pal-PMP22 is similar and both of them prefer to partition into the Ld domains enriched in DOPCs (data not shown).

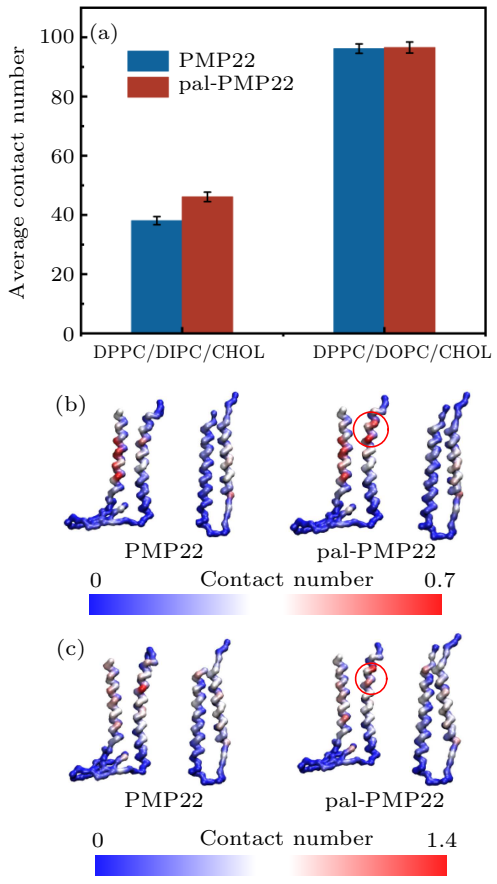


Fig. 3. (a) The contact number of PMP22 and pal-PMP22 with DPPCs and CHOLs in the Lo domains in two lipid bilayers with different compositions. The error bars represent the standard deviations. (b)–(c) Contact maps for the residues of PMP22 and pal-PMP22 with DPPCs and CHOLs in the lipid bilayers composed of (b) DPPC/DIPC/CHOL and of (c) DPPC/DOPC/CHOL. The position of the palmitoylation site is labeled with a red circle.

To examine the partitioning of PMP22/pal-PMP22 into the Lo domains, we analyzed the number of contacts of the proteins with DPPCs and CHOLs in the Lo domain of the two lipid bilayers as shown in Fig. 3(a). We find that the number of contacts between the proteins and DPPCs as well as CHOLs in the lipid bilayer of DPPC/DOPC/CHOL is obviously larger than that in the lipid bilayer of DPPC/DIPC/CHOL, indicating that the composition of the lipid bilayer has a significant impact on the partitioning of the proteins into the Lo domains. Additionally, as shown in Fig. 3(a), we also find that pal-PMP22 exhibits a higher affinity with the Lo domain than PMP22 in the bilayer of DPPC/DIPC/CHOL while they show a similar affinity with the Lo domain in the bilayer of DPPC/DOPC/CHOL. Furthermore, the contacting maps of PMP22/pal-PMP22 with the lipids shown in Figs. 3(b) and 3(c) illustrate the detailed interactions between the residues of the proteins and the lipids. In the bilayer of DPPC/DIPC/CHOL, the contacts between pal-PMP22 and DPPC/CHOL at the palmitoylated site (CYS85) obviously increase compared with the contacts between PMP22 and DPPC/CHOL. However, in the bilayer of DPPC/DOPC/CHOL, the contacts between the two proteins and DPPC/CHOL at the palmitoylated site are similar. Therefore, palmitoylation plays a significant role in the affinity of PMP22 with the Lo domain in the bilayer of DPPC/DIPC/CHOL while it has a negligible effect on the partitioning of PMP22 in the bilayer of DPPC/DOPC/CHOL.

To thermodynamically understand the partitioning of PMP22/pal-PMP22 into the lipid domains, we calculated the PMF profiles of the proteins and the phase-separated lipid bilayer as shown in Fig. 4. In the bilayer of DPPC/DIPC/CHOL as shown in Fig. 4(a), the minimum of the PMF profile of the PMP22 is located at the center of the Ld domain, indicating that the protein prefers to partition into the Ld domain. For pal-PMP22, the minima of the PMF profile localize at the boundary of the Lo and Ld domains, as illustrated by the inset, indicating that pal-PMP22 prefers to be located at the boundary of the lipid domains. In addition, the difference of the PMF for PMP22 partitioning into the Lo and Ld domains is

larger than the difference of the PMF for pal-PMP22 partitioning into the Lo and Ld domains, which implies that palmitoylation increases the possibility of PMP22 partitioning into the Lo domain. In the bilayer of DPPC/DOPC/CHOL as shown in Fig. 4(b), however, the difference in the PMF profiles for PMP22 and pal-PMP22 partitioning into the lipid domains is negligible, indicating that both the proteins primarily prefer to partition into the Ld domain and palmitoylation has little effect on the partitioning of PMP22 into the lipid domains.

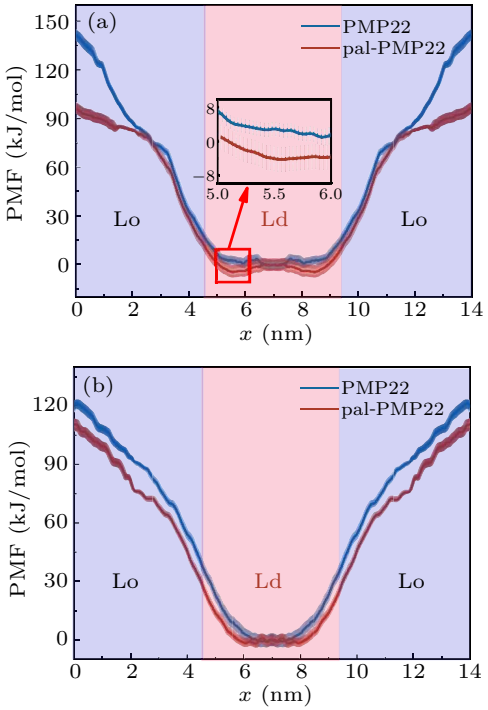


Fig. 4. PMF profiles of PMP22 and pal-PMP22 in the pre-separated Lo–Ld–Lo lipid bilayers composed of (a) DPPC/DIPC/CHOL and of (b) DPPC/DOPC/CHOL. The error bars are shown with shadows.

3.2. Palmitoylation-induced tilt of PMP22 enhances its affinity with Lo domain

To gain a microscopic understanding of how palmitoylation affects the partitioning of PMP22 into lipid domains, we analyzed the tilting angle of PMP22 and pal-PMP22 relative to the bilayer normal, as illustrated in Fig. 5. The tilting angles dynamically vary throughout the simulations and exhibit a Gaussian-like distribution. In the bilayer of DPPC/DIPC/CHOL, the peak of the distribution of the tilting angle of pal-PMP22 is obviously larger than that of PMP22 as shown in Fig. 5(a), suggesting that palmitoylation enhances the tilt of PMP22 in the lipid bilayers. This result is also consistent with the snapshots shown in Fig. 2 where pal-PMP22 is obviously tilted in the lipid bilayer in most of the simulation time. Additionally, as shown in Fig. 2, PMP22 and pal-PMP22 mainly partition into the Ld domain which has a relatively small hydrophobic thickness.[60–62] Therefore, the larger tilting angle of pal-PMP22 indicates that the hydrophobic palmitic acid chain in the pal-PMP22 increases the hydrophobic thickness of the proteins, inducing a larger hydrophobic mismatch between the protein and the Ld domain. The Lo domain, with a larger hydrophobic thickness, matches the hydrophobic thickness of pal-PMP22 better than the Ld domain. Consequently, pal-PMP22 shows an affinity with the Lo domain or tends to localize at the boundary of the Lo/Ld domains as indicated by the PMF profile in Fig. 4(a) with the influence of the hydrophobic mismatch effect.

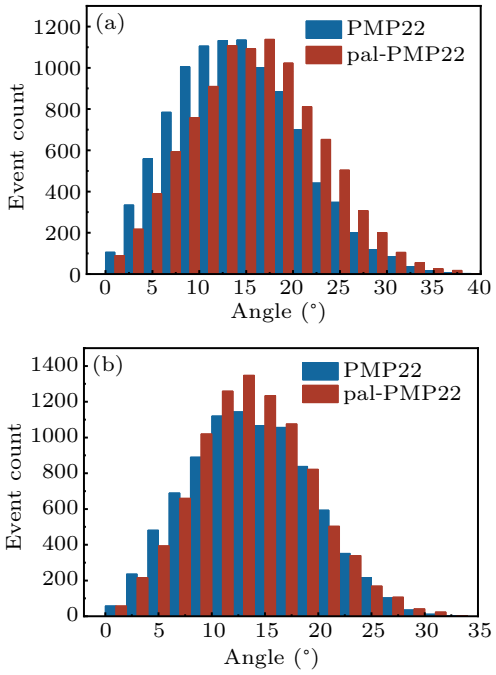


Fig. 5. The distribution of tilting angles of PMP22 and pal-PMP22 in the lipid bilayers composed of (a) DPPC/DIPC/CHOL and of (b) DPPC/DOPC/CHOL.

In the bilayer of DPPC/DOPC/CHOL, however, since the degree of unsaturation of DOPC is small, the hydrophobic thickness of the Ld domain is comparable to that of the Lo domain. Thus, the tilting angles of PMP22 and pal-PMP22 are comparable as shown in Fig. 5(b). Consequently, in the bilayer of DPPC/DOPC/CHOL, the hydrophobic mismatch effect is not so significant as in the bilayer of DPPC/DOPC/CHOL and has a negligible effect on the protein partitioning into the Lo domain, which provides one of the possible microscopic mechanisms for the PMF profile shown in Fig. 4(b).

3.3. Palmitoylation influences the packing order of lipids.

We further examined the packing order of lipid tails to understand the effect of palmitoylation on the partitioning of PMP22 into the lipid domains, as shown in Fig. 6. In the lipid bilayers of DPPC/DIPC/CHOL, the order parameters of DIPCs are nearly identical in the bilayer inserted with PMP22 and pal-PMP22 as shown in Fig. 6(a), indicating that the palmitic acid chain has no influence on the packing order

of DIPC. However, the order parameter of DPPC obviously increases in the bilayer inserted with pal-PMP22, compared with that in the bilayer inserted with PMP22 (Fig. 6(b)). Therefore, the palmitic acid chain enhances the ordered packing of DPPC in the Lo domain. The different influences of the palmitic acid chain on the packing order of DIPCs and DPPCs may be a crucial factor for promoting pal-PMP22 to be located at the boundary of the Lo/Ld domains or partition into the Lo domain in the lipid bilayer of DPPC/DIPC/CHOL as illustrated by the PMF in Fig. 4(a).

However, in the lipid bilayer of DPPC/DOPC/CHOL, as illustrated in Figs. 6(c) and 6(d), both the order parameters of DOPCs and DPPCs are barely influenced by the palmitic acid chain and they are identical in the bilayers inserted with pal-PMP22 and PMP22. Thus, both PMP22 and pal-PMP22 prefer to partition into the Ld domain enriched in DOPCs as indicated by the PMF in Fig. 4(b).

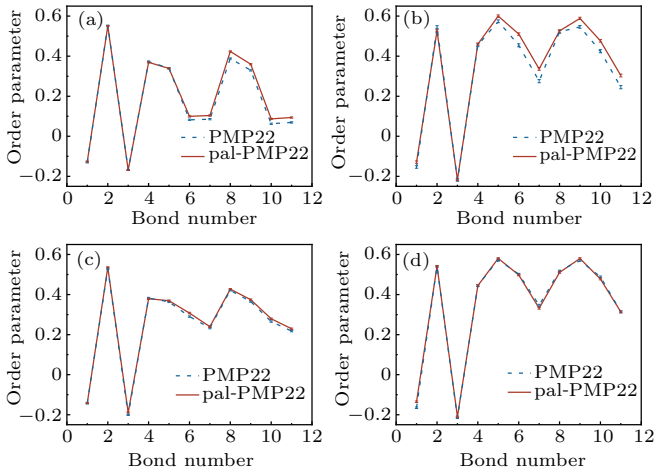


Fig. 6. (a)–(b) Order parameters of (a) DIPC and (b) DPPC in the lipid bilayers composed of DPPC/DIPC/CHOL with the influences of PMP22 and pal-PMP22. (c)–(d) Order parameters of (c) DOPC and (d) DPPC in the lipid bilayers composed of DPPC/DOPC/CHOL with the influences of PMP22 and pal-PMP22. The error bars represent the standard deviations.

4. Conclusions

In this work, we employed coarse-grained MD simulations to study the effect of palmitoylation on the partitioning of PMP22 protein into the Lo and Ld domains in the phase-separated lipid bilayers. The results indicate that both PMP22 and pal-PMP22 primarily favor to partition into the Ld domains in both the lipid bilayers composed of DPPC/DIPC/CHOL and DPPC/DOPC/CHOL, which agrees well with the experimental results in the GUV. However, the palmitic acid chain in the pal-PMP22 still exhibits varying impacts on the PMP22 partitioning into the lipid domains in the two different lipid bilayers. In the bilayer of DPPC/DIPC/CHOL, palmitoylation significantly increases the tilt of PMP22 in the Ld domain and the order parameter of DPPC in the Lo domain, driving pal-PMP22 to localize at the boundary of the Lo and Ld domains. Nevertheless, in the bilayer of DPPC/DOPC/CHOL, the effect of palmitoylation on the partitioning of PMP22 into the lipid domains is not so significant as that in the bilayer of DPPC/DIPC/CHOL. Therefore, the effect of palmitoylation on the PMP22 partitioning into the lipid domains depends on the compositions of the lipid bilayers, and this result is also consistent with the experimental results in the GPMV where pal-PMP22 prefers to partition into the Lo domains. The findings of this work provide some molecular insights into understanding the effect of palmitoylation on the interaction between PMP22 and myelin membranes as well as the physiological function of the protein.

Acknowledgements

Project supported by Zhejiang Provincial Natural Science Foundation of China (Grant No. LZ25A040005) and the National Natural Science Foundation of China (Grant No. 11674287). Computational resources provided by the Scientific Computing Center of Zhejiang Normal University are appreciated.

References

[1] Sezgin E, Levental I, Mayor S and Eggeling C 2017 *Nat. Rev. Mol. Cell Biol.* **18** 361
[2] Singer S J and Nicolson G L 1972 *Science* **175** 720
[3] Simons K and Ikonen E 1997 *Nature* **387** 569
[4] Ingólfsson H I, Melo M N, van Eerden F J, Arnarez C, Lopez C A, Wassenaar T A, Periole X, de Vries A H, Tieleman D P and Marrink S J 2014 *J. Am. Chem. Soc.* **136** 14554
[5] Levental I and Lyman E 2023 *Nat. Rev. Mol. Cell Biol.* **24** 107
[6] Goyette J and Gaus K 2017 *Curr. Opin. Cell Biol.* **44** 86
[7] Garcia-Parajo M F, Cambi A, Torreno-Pina J A, Thompson N and Jacobson K 2014 *J. Cell Sci.* **127** 4995
[8] Puff N 2023 *Membranes* **13** 652
[9] Moreno-Pescador G, Arastoo M R, Ruhoff V T, Chiantia S, Daniels R and Bendix P M 2023 *Nano Lett.* **23** 3377
[10] Kusumi A, Fujiwara T K, Tsunoyama T A, Kasai R S, Liu A A, Hirosawa K M, Kinoshita M, Matsumori N, Komura N, Ando H and Suzuki K G N 2020 *Traffic* **21** 106
[11] Lin X and Gorfe A A 2019 *J. Phys. Chem. B* **123** 1009
[12] Lorent J H, Diaz-Rohrer B, Lin X, Spring K, Gorfe A A, Levental K R and Levental I 2017 *Nat. Commun.* **8** 1219
[13] Lin X, Gorfe A A and Levental I 2018 *Biophys. J.* **114** 1936
[14] Balakrishnan M and Kenworthy A K 2024 *J. Am. Chem. Soc.* **146** 1374
[15] Jetten A M and Suteri U 2000 *Prog. Nucleic Acid Res. Mol. Biol.* **64** 97
[16] Snipes G J, Suter U, Welcher A A and Shooter E M 1992 *J. Cell Biol.* **117** 225
[17] Zhou Y, Miles J R, Tavori H, Lin M, Khoshbouei H, Borchelt D R, Bazick H, Landreth G E, Lee S, Fazio S and Notterpek L 2019 *J. Neurosci.* **39** 5404
[18] Stefanski K M, Wilkinson M C and Sanders C R 2024 *Biochem. So. Trans.* **52** 1747
[19] Prior R, Silva A, Vangansewinkel T, *et al*. 2024 *Brain* **147** 3113
[20] van Paassen B W, van der Kooi A J, van Spaendonck-Zwarts K Y, Verhamme C, Baas F and de Visser M 2014 *Orphanet. J. Rare Dis.* **9** 38
[21] Attarian S, Fatehi F, Rajabally Y A and Pareyson D 2020 *J. Neurol.* **267** 2198
[22] Taioli F, Cabrini I, Cavallaro T, Acler M and Fabrizi G M 2011 *Brain* **134** 608
[23] Li J, Parker B, Martyn C, Natarajan C and Guo J 2013 *Mol. Neurobiol.* **47** 673

[24] Saher G, Brügger B, Lappe-Siefke C, Möbius W, Tozawa R, Wehr M C, Wieland F, Ishibashi S and Nave K A 2005 *Nat. Neurosci.* **8** 468
[25] Gopalakrishnan G, Awasthi A, Belkaid W, De Faria O, Liazoghli D, Colman D R and Dhaunchak A S 2013 *J. Neurosci. Res.* **91** 321
[26] Marinko J T, Kenworthy A K and Sanders C R 2020 *Proc. Natl. Acad. Sci. USA* **117** 14168
[27] Schlebach J P, Narayan M, Alford C, Mittendorf K F, Carter B D, Li J and Sanders C R 2015 *J. Am. Chem. Soc.* **137** 8758
[28] Lee S, Amici S, Tavori H, Zeng W M, Freeland S, Fazio S and Notterpek L 2014 *J. Neurosci.* **34** 16140
[29] Mittendorf K F, Marinko J T, Hampton C M, Ke Z, Hadziselimovic A, Schlebach J P, Law C L, Li J, Wright E R and Sanders C R 2017 *Sci. Adv.* **3** e1700220
[30] Zoltewicz S J, Lee S, Chittoor V G, Freeland S M, Rangaraju S, Zacharias D A and Notterpek L 2012 *ASN Neuro.* **4**
[31] Li S, Li J, Ning L, Wang S, Niu Y, Jin N, Yao X, Liu H and Xi L 2015 *J. Chem. Inf. Model* **55** 2015
[32] Schlebach J P, Barrett P J, Day C A, Kim J H, Kenworthy A K and Sanders C R 2016 *Biochemistry* **55** 985
[33] Wang T Y, Leventis R and Silvius J R 2001 *Biochemistry* **40** 13031
[34] Uchida K, Obayashi H, Minamihata K, Wakabayashi R, Goto M, Shimokawa N, Takagi M and Kamiya N 2022 *Langmuir* **38** 9640
[35] Marrink S J, Corradi V, Souza P C T, Ingólfsson H I, Tieleman D P and Sansom M S P 2019 *Chem. Rev.* **119** 6184
[36] Marrink S J, Risselada H J, Yefimov S, Tieleman D P and de Vries A H 2007 *J. Phys. Chem. B* **111** 7812
[37] Borges-Araújo L, Borges-Araújo A C, Ozturk T N, Ramirez-Echemendia D P, Fábián B, Carpenter T S, Thallmair S, Barnoud J, Ingólfsson H I, Hummer G, Tieleman D P, Marrink S J, Souza P C T and Melo M N 2023 *J. Chem. Theory Comput.* **19** 7387
[38] Souza P C T, Alessandri R and Barnoud J, *et al.* 2021 *Nat. Methods* **18** 382
[39] Wu Q Y and Liang Q 2014 *Langmuir* **30** 1116
[40] Lin X, Chen X J and Liang Q 2021 *Chin. Phys. B* **30** 068701
[41] Chen X J and Liang Q 2017 *Chin. Phys. B* **26** 048701
[42] Chen J, Tieleman D P and Liang Q 2022 *J. Phys. Chem. Lett.* **13** 991
[43] de Jong D H, Singh G, Bennett W F, Arnarez C, Wassenaar T A, Schäfer L V, Periole X, Tieleman D P and Marrink S J 2013 *J. Chem. Theory Comput.* **9** 687
[44] Lin X, Chen X J and Liang Q 2021 *Chin. Phys. B* **30** 068701
[45] Chen X J and Liang Q 2017 *Chin. Phys. B* **26** 048701
[46] Jo S, Kim T, Iyer V G and Im W 2008 *J. Comput. Chem.* **29** 1859
[47] Koukos P I, Dehghani-Ghahnaviyeh S, Velez-Vega C, Manchester J, Tieleman D P, Duca J S, Souza P C T and Cournia Z 2023 *J. Chem. Theory Comput.* **19** 8901
[48] Wassenaar T A, Ingólfsson H I, Böckmann R A, Tieleman D P and Marrink S J 2015 *J. Chem. Theory Comput.* **11** 2144
[49] Li W, Lin Z, Yuan B and Yang K 2020 *Chin. Phys. B* **29** 128701
[50] Abraham M J, Murtola T, Schulz R, Páll S, Smith J C, Hess B and Lindahl E 2015 *SoftwareX* **1** 19
[51] Bussi G, Donadio D and Parrinello M 2007 *J. Chem. Phys.* **126** 014101
[52] Berendsen H J C, Postma J P M, van Gunsteren W F, DiNola A and Haak J R 1984 *J. Chem. Phys.* **81** 3684
[53] Park S, Yeom M S, Andersen O S, Pastor R W and Im W 2019 *J. Chem. Theory Comput.* **11** 6491
[54] Domański J, Hedger G, Best R B, Stansfeld P J and Sansom M S P 2016 *J. Phys. Chem. B* **121** 3364
[55] Souaile M and Roux B 2001 *Comput. Phys. Commun.* **135** 40
[56] Hub J S, de Groot B L and van der Spoel D 2010 *J. Chem. Theory Comput.* **6** 3713
[57] Efron B 1979 *Ann. Statist.* **7** 1
[58] Zhu F and Hummer G 2012 *J. Comput. Chem.* **33** 453
[59] Humphrey W, Dalke A and Schulten K 1996 *J. Mol. Graph* **14** 33
[60] Kim T and Im W 2010 *Biophys. J.* **99** 175
[61] Andersen O S and Koeppe R E II 2007 *Annu. Rev. Biophys. Biomol. Struct.* **36** 107
[62] Liang Q, Wu Q Y and Wang Z Y 2014 *J. Chem. Phys.* **141** 074702